[Supplementary Material] High-resolution long-term average groundwater recharge in Africa estimated using random forest regression and residual interpolation

Anna Pazola[1,2], Mohammad Shamsudduha[3], Jon French[1], Alan M. MacDonald[4], Tamiru Abiye[5], Ibrahim Baba Goni[6], and Richard G. Taylor[1]

[1]Department of Geography, University College London, Gower St, London WC1E 6BT, United Kingdom
[2]United Nations Environment Programme World Conservation Monitoring Centre, 219 Huntingdon Road, Cambridge CB3 0DL, United Kingdom
[3]Institute for Risk & Disaster Reduction, University College London, Gower St, London WC1E 6BT, United Kingdom
[4]British Geological Survey, Lyell Centre, Research Avenue South, Edinburgh EH14 4AP, United Kingdom
[5]School of Geosciences, University of the Witwatersrand, 1 Jan Smuts Ave, Braamfontein, Johannesburg 2000, South Africa
[6]Department of Geology, University of Maiduguri, 1069 Bama - Maiduguri Rd, 600104, Maiduguri, Nigeria

Correspondence: Anna Pazola (anna.pazola.20@ucl.ac.uk)

1.   Workflow

Figure S1 illustrates the steps undertaken to derive groundwater recharge estimates using a data-driven method and compare them with the modelling results obtained from a linear mixed model by MacDonald et al. (2021). Most steps are sequential, with their outputs feeding the subsequent actions.
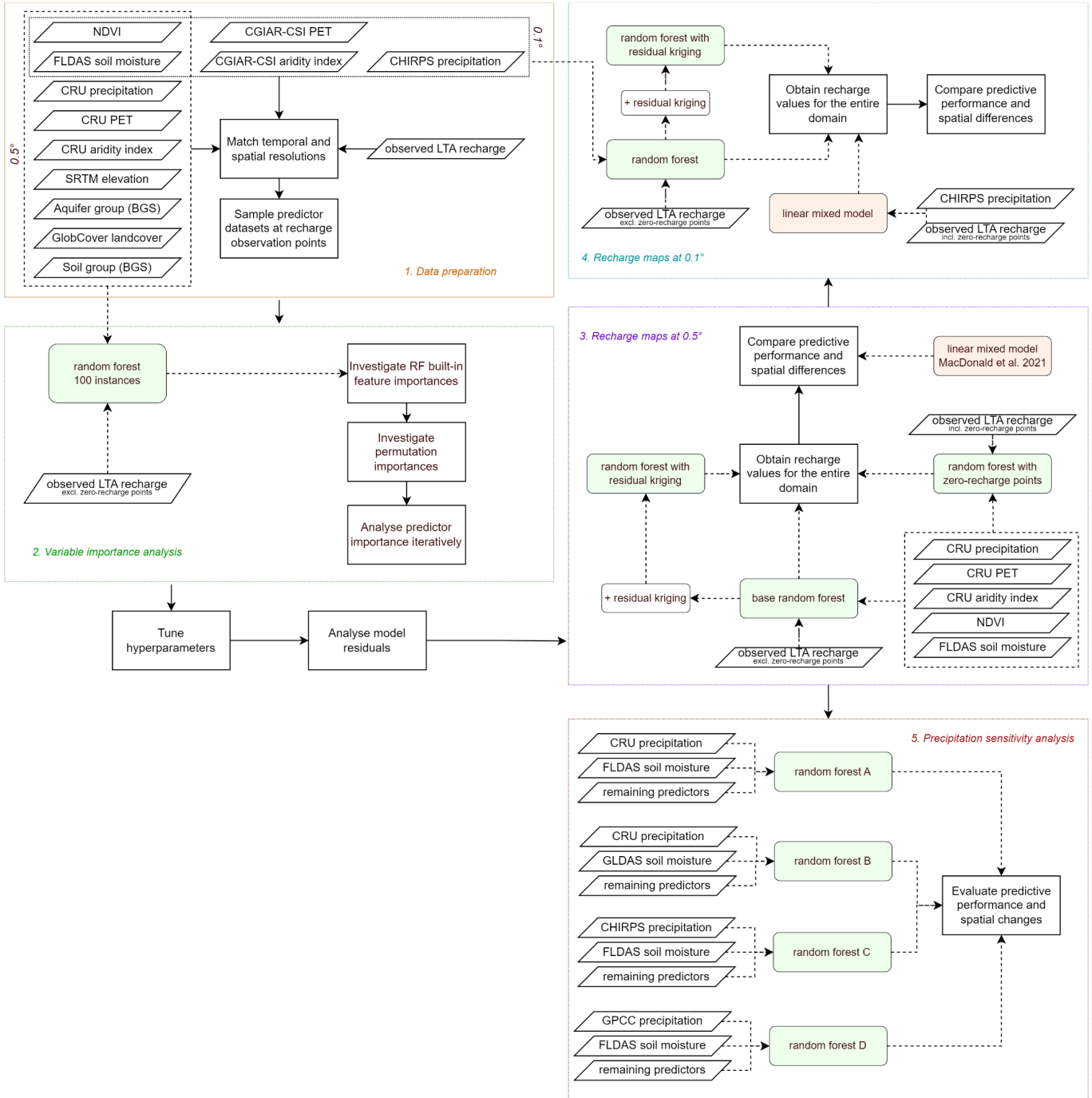

Figure S1. Flow diagram showing the steps performed in this analysis to achieve research goals.

2. Details on input data

Table S1. Summary of gridded datasets used in this study. Each input raster was upscaled using bilinear (continuous data) or mode (categorical data) resampling methods to an appropriate resolution (0.5° x 0.5° or 0.1° x 0.1°) before being applied in the random forest model. Long-term averages for the indicated time period were extracted from time series datasets.

| Name	Type	Units	Spatial resolution	Time period	Data sources	Used for
Explanatory variables						
Precipitation	Continuous point data	mm/yr	0.5° × 0.5°	1981–2010	CRU TS climate dataset (Harris et al., 2020)	predictor analysis 0.5° recharge map, sensitivity analysis,
			0.05° × 0.05°	1981-2010	CHIRPS (Funk, Peterson, et al., 2015)	0.1° recharge map, sensitivity analysis
			0.5° × 0.5°	1981-2010	GPCC (Schneider et al., 2011)	sensitivity analysis
Potential evapotranspiration	Continuous point data	mm/yr	0.5° × 0.5°	1981–2010	CRU TS climate dataset (Harris et al., 2020)	predictor analysis, 0.5° recharge map
			30 arc-seconds	1970-2000	CGIAR-CSI (Trabucco and Zomer, 2019)	0.1° recharge map
Aridity index	Continuous point data	-	0.5° × 0.5°	1981–2010	CRU TS climate dataset (Harris et al., 2020)	predictor analysis, 0.5° recharge map
			30 arc-seconds	1970-2000	CGIAR-CSI (Trabucco and Zomer, 2019)	0.1° recharge map
Soil moisture	Continuous point data	kg/m²	0.25° × 0.25°	1981-2010	GLDAS Noah LSM L4 (Beaudoing and Rodell, 2019)	sensitivity analysis
		m³/m³	0.1° × 0.1°	1982-2010	FLDAS Noah LSM L4 (McNally, 2018)	predictor analysis, 0.5° and 0.1° recharge maps, sensitivity analysis
NDVI	Continuous point data	-	0.05° × 0.05°	1981-2010	Personal communication, British Geological Survey, derived from Didan et al., 2015	predictor analysis, 0.5° and 0.1° recharge maps
Aquifer group	Categorical data	-	-	-	Personal communication, British Geological Survey (MacDonald et al., 2012)	predictor analysis
Soil group	Categorical data	-	-	-	Personal communication, British Geological Survey, derived from Jones et al., 2013	predictor analysis
Landcover	Categorical data	-	approx. 300 m	2009	GlobCover (Arino et al., 2007)	predictor analysis, 0.5° and 0.1° recharge maps
Elevation	Continuous point data	m	approx. 90 m	-	SRTM 90m DEM (Jarvis et al., 2008)	predictor analysis, 0.5° and 0.1° recharge maps
Dependent variable						
Groundwater recharge	Continuous point data	mm/yr	0.5° × 0.5°	1970-2019	Dataset by MacDonald et al., 2020	model training and testing
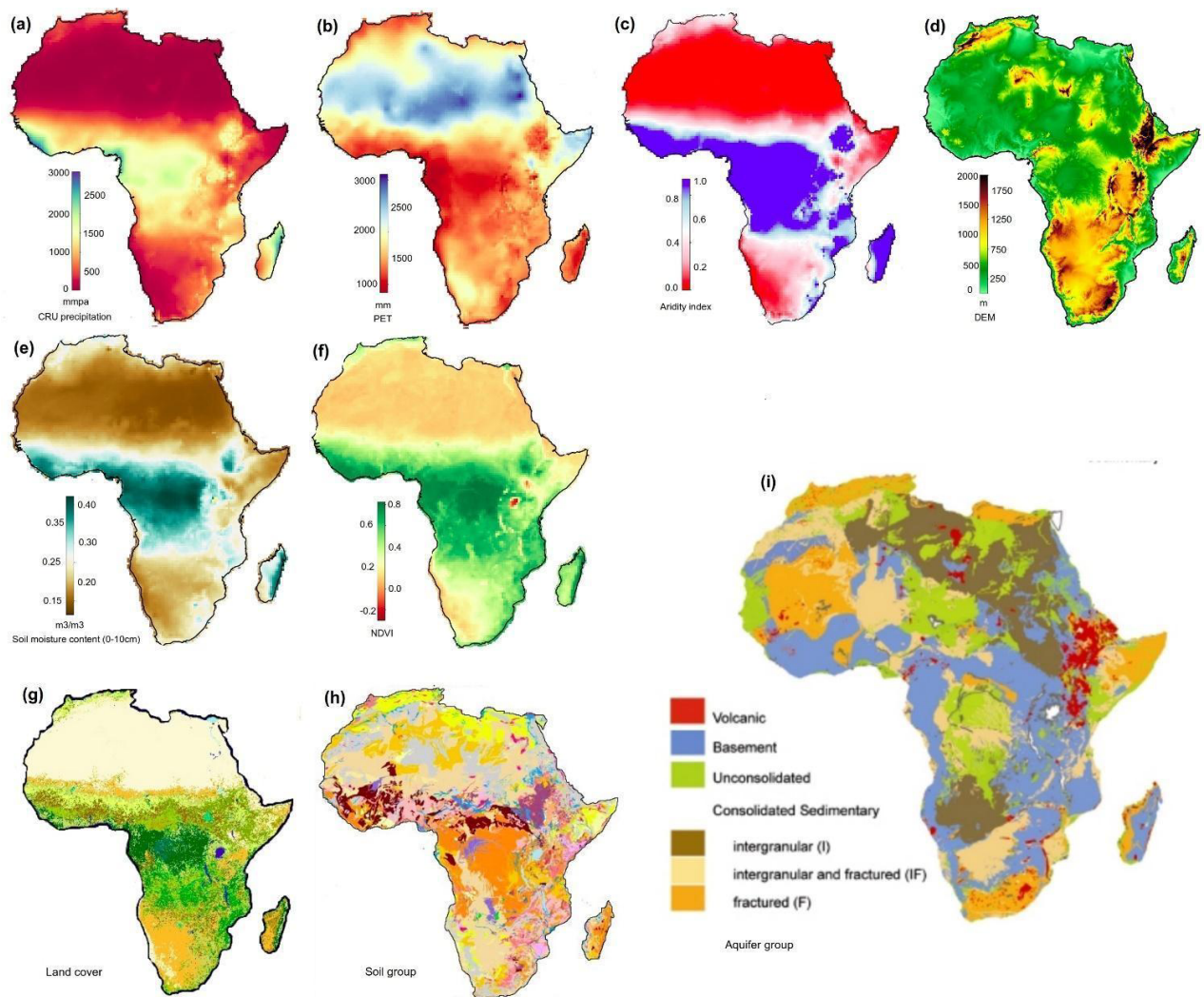
Figure S2. Spatial distribution of groundwater recharge predictors across Africa used in the initial predictor importance analysis: (a) precipitation (mm/year), (b) evapotranspiration (mm), (c) aridity index, (d) elevation (m), (e) soil moisture (m^3/m^3), (f) NDVI, (g) landcover, (h) soil group (graphic source: Soil Atlas of Africa, Jones et al. (2013)), (i) aquifer group (graphic source: MacDonald et al. (2012)). See Table S1 for details on data sources.
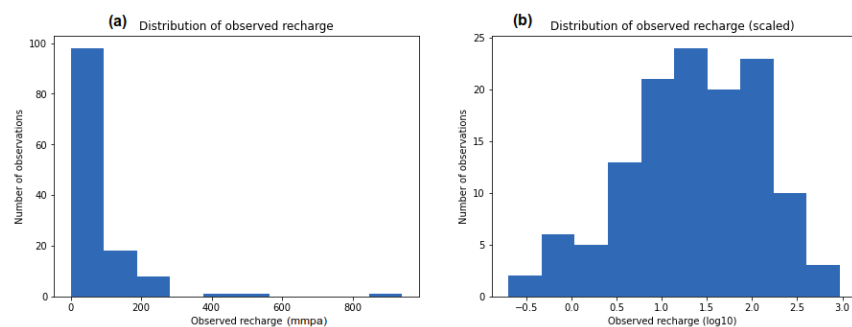

Figure S3. Distribution of observed groundwater recharge in the sample set of 127 observations in the original (linear) scale (a) and in the log scale (b), transformed by applying the common logarithm.

3.   Linear Mixed Model (LMM)

A LMM was developed at 0.1° to allow for a comprehensive comparison of models at both spatial resolutions of 0.5° and 0.1°. To keep the LMM at 0.1° consistent with the model at 0.5° developed by MacDonald et al. 2021, the predictor importance analysis was omitted and only one covariate – precipitation - is used as the input to the statistical model. The optimal parameters of the fixed and random effects are listed in Table S2.

Table S2: Optimal LMM parameters for fixed and random effects at 0.1°.

Fixed effects parameters		
Parameter	*Estimate*	*Standard error*
β_0	-2.79	0.598
β_1	0.98	0.100

Random effects parameters	
κ	0.5
c_0	0.53
c_1	1.217
φ	645.49

The fixed effects model is represented by the following equation:

$$log_e(LTA\_recharge) = \beta_0 + \beta_1 log_e(LTA\_rainfall)$$

and the random effects are the independently and identically distributed error c_0 and a spatially correlated Gaussian random field modelled with Matern correlation function. For more details, refer to Supplementary Material of MacDonald et al. 2021.

4.   Residual kriging for Random Forest

Kriging-type interpolation of residuals is also applied on top of the prediction results from the RF model to explicitly account for spatial variability in LTA recharge observations around the fitted values, under the assumption that the LTA recharge observations are likely to be similar for all unsampled sites in the proximity to the sampled sites. Contrary to the LMM residuals that were kriged as a part of E-BLUP procedure for LMM, RF residuals exhibit low spatial dependence and low semivariance. As a result, the effect of residual kriging on the final prediction values was localised.

Table S3: Ordinary Kriging parameters for kriging-type interpolation of random forest residuals at 0.5° and 0.1°. Spherical model was used as the variogram model, that was fitted to unprojected residuals, using great-circle distances, returning km as units.

Kriging parameters		
	0.5°	0.1°
c_0	0.059	0.04
c_1	0.021	0.024
φ	237.73	250.52

5.   Additional analysis: random forest

5.1.   *Variable importance*

Random forest regressor works as a black-box model since its internal decision trees cannot be examined individually and no regression coefficients are calculated by the model. However, it generates information on variable importance that can be compared to other regression techniques. It is an important feature when working with high dimensional data since the variable selection can be a time-consuming, error-prone, and subjective task. The generation method depends on the implementation of the random forest regressor. In the Python implementation used in this study, the importance of a variable is expressed in terms of the Gini importance and it measures the decrease in the impurity of the split in an internal node for that feature. It is computed as the normalised total reduction in the variance brought by that variable.

The variable importance experiment utilised 100 random forest models grown using all explanatory variables listed in Table S1. Prior to inspecting the variable importance, the predictive performance of the models was checked to ensure their predictive power was satisfactory. The R^2 values of training and testing sets ranged between 0.93-0.95 and 0.42-0.81 respectively. The oob score oscillated between 0.58-0.70. Then, the feature importance information was averaged over all models. Based on the RMSE performance metric, the best model was selected out of the ensemble and its variable importance was compared with the obtained mean. **The mean of the built-in impurity-based feature importances over all models revealed that precipitation, soil moisture, aridity index and NDVI have the most explanatory power, as illustrated in Figure S5.**
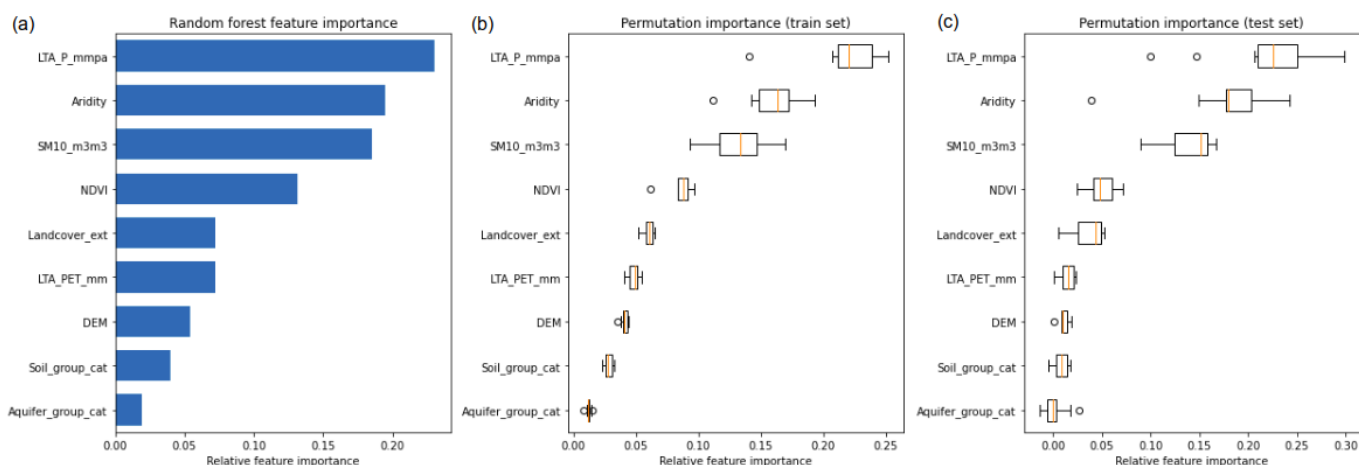

Figure S5. Relative feature importance obtained using the random forest-specific score of the total reduction in the variance brought by a variable (a), and using a model agnostic permutation importance of features based on training dataset (b) and testing dataset (c). Results generated using Python implementation of RandomForestRegressor and permutation_importance method from scikit-learn version 0.24.2.

Although this method can deliver valuable information at no extra computational cost, impurity-based importances exhibit a bias towards variables of high cardinality. Furthermore, they do not reflect the ability of a variable to make generalised predictions with respect to the testing set, as they are based on training set statistics (Parr et al. (2018)). Thus, an additional permutation importance analysis was carried out. The permutation feature importance is expressed as the decline in a model score when a single input variable is randomly shuffled. This breaks the input-output relationship and allows an assessment of how much the target value depends on the particular feature. The chosen method *permutation_importance* from the sklearn library was applied to a single fitted random forest model and the features were shuffled 30 times. As illustrated in Figure S5, it was confirmed that the aforementioned variables have the highest explanatory power but their ranking might vary between the individual models due to the random factor. This large variance suggests that the top variables are highly correlated as the substitution of one variable through another does not considerably affect the model performance. Permutation importance analysis applied to the testing set did not indicate any significant differences in the ranking of the variable importance.

However, in the case of highly correlated predictor variables, both impurity-based feature importance and permutation importance can lead to incorrect conclusions as they can falsely classify one variable as truly important, while it might hold predictive value mainly because of the correlation with another essential variable. Although multicollinearity of variables does not affect the predictive power of the model, an additional iterative importance analysis based on the adjusted R^2 metric was

carried out to identify the real influence of variables on the model. First, the variable clusters were identified using hierarchical clustering based on the Spearman rank-order correlations. The Spearman rank-order correlation coefficient is a non-parametric measure of the strength and direction of the relationship between two variables. Hierarchical clustering procedure groups highly collinear variables based on Spearman rank-order correlations under a given threshold. Its results are illustrated in Figure S6. When applied to the predictors set, it identified two strong clusters of correlated variables: (1) precipitation, soil moisture, aridity and NDVI, (2) potential evapotranspiration and landcover.
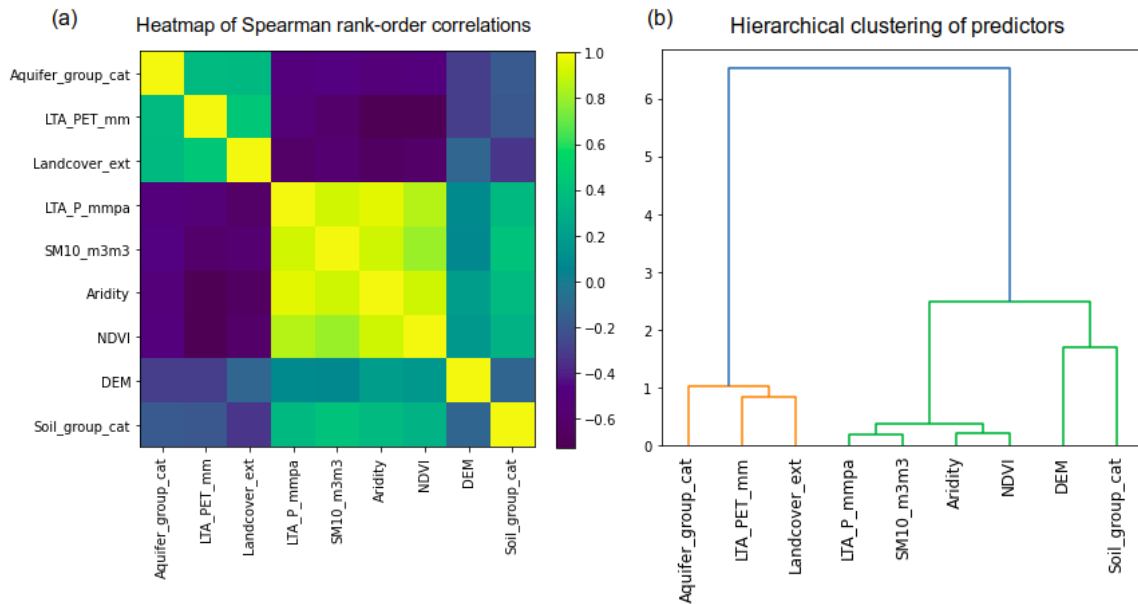

Figure S6. Spearman rank-order correlation heatmap (a) and corresponding hierarchical clustering (b) for detecting highly correlated variables. Given the threshold=1, two variable clusters are identified: (1) precipitation, soil moisture, aridity and NDVI, and (2) potential evapotranspiration and landcover.

This analysis built a basis for a further iterative variable importance investigation using random forest. Due to the random character of the growing process, multiple random forest models were built with a fixed random state parameter and using the same training and testing datasets to allow comparability of individual models and attribute any changes in model performance to the explanatory power of selected variables. Adjusted R^2 was used as a performance metric to decide whether a given variable should be kept in the model. Iterative variable selection was performed as follows: the first model was built with the strongest predictor - precipitation - only. Next, one variable from each cluster was picked and used to grow a new model together with other variables already recognised as important. Finally, the remaining correlated variables were added to the predictor set one at a time to check whether any additional performance increase could be observed. The detailed results are presented in Table S1.

Table S4. Sequence of random forest models for LTA groundwater recharge with corresponding adjusted R² performance metrics under a varying set of independent variables. Variables are added iteratively and are kept in the predictor set if they lead to a performance improvement.

Variables considered	Training set R^2_{adj}	Testing set R^2_{adj}	Kept?
Precipitation	0.91	0.67	Yes
Precipitation + PET	0.93	0.73	Yes
Precipitation + PET + DEM	0.92	0.73	No
Precipitation + PET + Aquifer Group	0.92	0.73	No
Precipitation + PET + Soil Group	0.93	0.73	No
Precipitation + PET + Aridity	0.94	0.73	Yes
Precipitation + PET + Aridity + NDVI	0.94	0.78	Yes
Precipitation + PET + Aridity + NDVI + Soil moisture	**0.94**	**0.79**	Yes
Precipitation + PET + Aridity + NDVI + Soil moisture + Landcover	0.94	0.78	No
All predictors	0.93	0.74	-

In summary, five variables contributed to a performance increase, with precipitation and potential evapotranspiration having a dominant influence on model performance. Aridity index, NDVI and soil moisture, all correlated with precipitation, had a marginal positive impact on the model whereas elevation, aquifer group, soil group and landcover did not benefit the model.

The results of the variable importance analysis confirmed that precipitation explains a large part of variance in the modelled LTA groundwater recharge, both directly and indirectly through the correlated variables. The inclusion of other meteorological and vegetation variables such as PET, aridity index, NDVI and soil moisture led to an improvement in the model fit, though often only a minor one, which is partially contrary to the findings of MacDonald et al. (2021), who did not find any statistically significant improvement in the recharge modelling from adding additional explanatory factors to the linear mixed model. It might suggest that the random forest model has a better ability to capture the underlying non-linear relationships between the explanatory factors and the target variable. In general, the findings of this study are consistent with broader research, in particular with Mohan et al. (2018), who lists the aforementioned variables as the most influential for groundwater recharge. Interestingly, subsurface factors had a marginal power in explaining variance in the target variable. It does not imply that the soil and aquifer group variables do not play any role in the groundwater recharge but rather that these particular parameters were not as relevant for the model as the climatic and vegetation factors. However, by employing a limited range of hydrogeological variables and thus implicitly assuming the homogeneity of subsurface properties, the random forest model might have missed important factors and consequently oversimplify the relationship between climate and groundwater recharge, which is a known issue in GHMs (De Vries and Simmers (2002); Hartmann et al. (2017)). High residual values for the data points located in the Gulf of Guinea and in DR Congo suggest that the model is not able to create a link between the current set of predictors and a few very high recharge observations. The incorporation of yet unidentified factors representing subsurface heterogeneity could possibly improve the prediction accuracy of the model for these points and effectively allow to incorporate focused recharge that is crucial to accurately assess the renewability of groundwater resources in the semi-arid regions but would require a significant amount of data engineering.

5.2. Precipitation sensitivity analysis

As the major influence of precipitation data on the dependent variable might lead to some variability in model output depending on the precipitation dataset, two other long-term rainfall datasets are employed in the precipitation sensitivity analysis to compare the modelled recharge under varying precipitation signal and quantify the corresponding output uncertainty. These precipitation datasets are derived from Climate Hazards Group InfraRed Precipitation with Station data (CHIRPS) version 2 at a spatial resolution of 0.05°, and Global Precipitation Climatology Centre (GPCC) Full Data Monthly Product version 2020 at a spatial resolution of 0.5°. CHIRPS data is produced by combining models of terrain-induced precipitation enhancement with interpolated ground-based station data and gridded satellite-based precipitation estimates from NASA and NOAA (Funk et al. (2015)). This blended approach overcomes issues of the lack of rain-gauge stations in rural regions and the satellite bias due to complex terrain leading to underestimating extreme rainfall events. The GPCC data is obtained from quality-controlled

observations collected from in-situ gauge stations (Schneider et al. (2011)). Compared to CRU TS dataset, GPCC uses substantially more observing stations.

The following settings were identified for the precipitation sensitivity analysis, each altering one of the rainfall-derived features of the input data:

- CRU precipitation + FLDAS soil moisture,
- CHIRPS precipitation,
- GPCC precipitation,
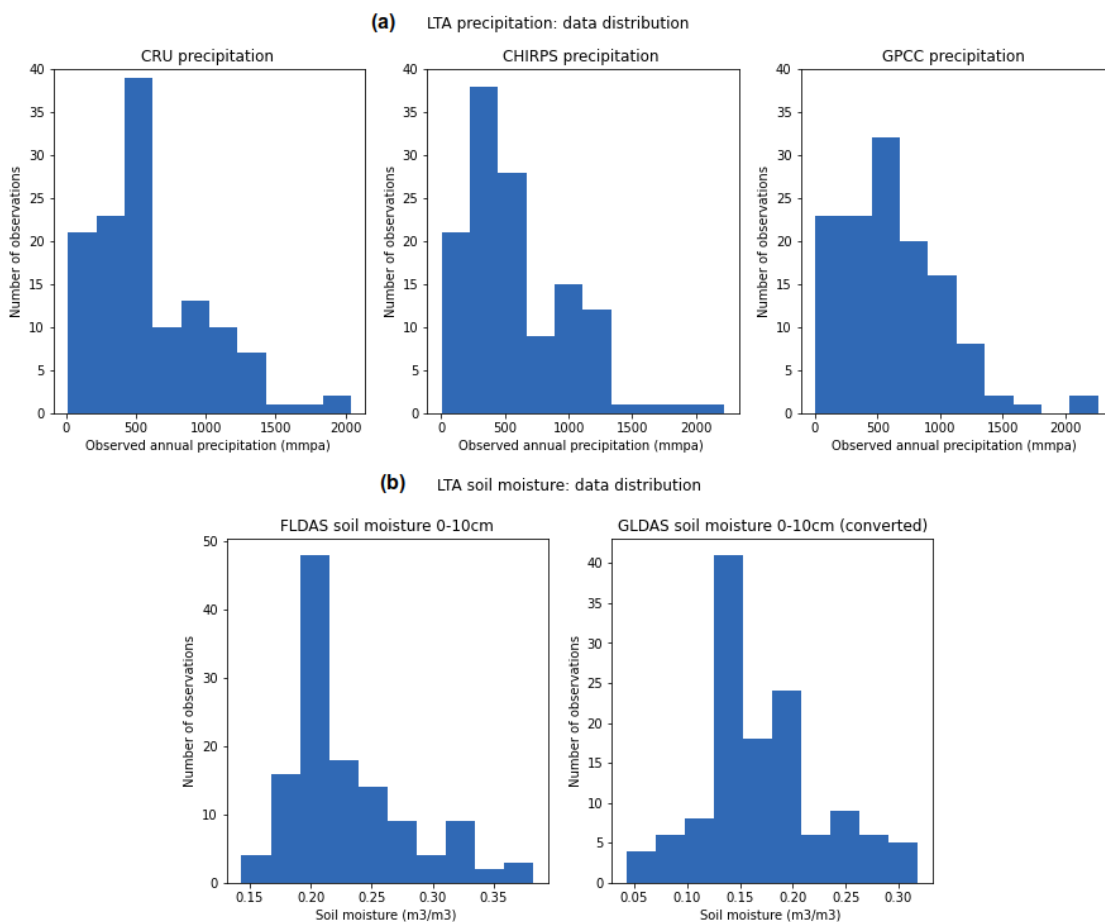- CRU precipitation + GLDAS soil moisture.

Figure S7. Comparison of the distribution of precipitation (a) and soil moisture (b) variables derived from different sources in the groundwater recharge sample set.

Figure S7 illustrates the distribution of each variable in the groundwater recharge dataset, excluding zero-recharge samples. There are some minor differences in the distribution of rainfall across different sources, notably in the semi-arid (400-600 mm/year) and in the sub-humid (600-1000 mm/year) areas. The soil moisture variables can be compared directly after the conversion of units, as the FLDAS product expresses soil moisture content on a volume basis (m^3/m^3), whereas the GLDAS derived values are measured on a weight basis (kg/m^2). The conversion is performed by dividing the values expressed on a weight basis by the assumed density of the water in the soil ($1000 \ kg/m^3$) and the thickness of the layer (10 cm).

To examine the influence of different precipitation datasets on the model performance and to allow an unbiased comparison of the individual precipitation data, a set of 4 models for each option was created in 100 iterations, amounting to 400 models in total, with a fixed random state (training/testing data selection, randomness of model building) in each iteration. In this analysis, the hyperparameters of each ensemble were not tuned to examine the direct impact of input dataset on the recharge predictions. The mean R^2 values and out-of-bag scores of the ensembles of 100 random forest models for each variant of the input dataset are summarised in Table S5 and indicate that there are minor differences in the performance of the model under varying input precipitation.

Table S5. Mean performance of an ensemble of 100 random forest models for each input data variant. The metrics are calculated based on output data in the log-scale.

Input data	R^2 train	R^2 test
CRU +FLDAS	0.95	0.61
CHIRPS	0.86	0.61
GPCC	0.95	0.66
CRU +GLDAS	0.94	0.60

However, as illustrated in Figures S8 and S9, there are some significant spatial differences in the predicted recharge between the original model output based on CRU precipitation and FLDAS soil moisture, and the model based on GPCC precipitation. In some areas of Central Africa, the recharge might differ by up to 150 mm/year. Notably, high relative differences are present in the Sahel belt, where the base model estimates oscillate between 1-2 mm/year, whereas the GPCC-based model predictions reach up to 7 mm/year. Notably, lower recharge rates are projected in the Maghreb by the latter model. The comparison of the base model values and the GLDAS based model identifies yet other areas of recharge prediction discrepancy. In East Africa, in Kenya and Tanzania, the increase in recharge may reach up to 130% when compared to the base model values. Although still very high, recharge values in the most humid areas of West Africa, the Gulf of Guinea and Madagascar, as well as in the heart of Africa, vary by as much as 100-200 mm/year. Most of these regions are areas with no direct recharge observations, hence a high variability.

Interestingly, CHIRPS and CRU precipitation datasets did not result in any significant spatial recharge differences.
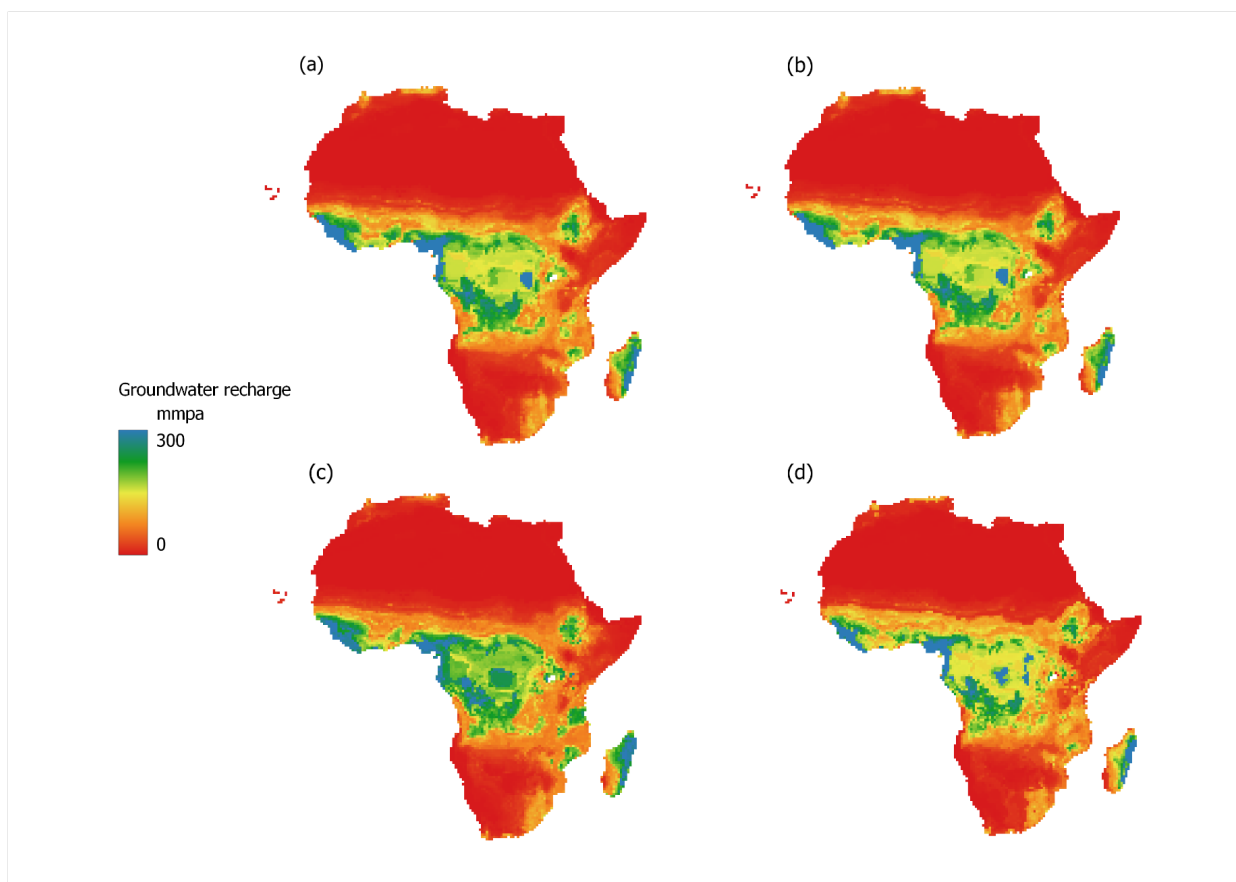
Figure S8. Comparison of modelled groundwater recharge using different precipitation and soil moisture datasets at a spatial resolution of 0.5°: (a) CRU precipitation + FLDAS soil moisture; (b) CHIRPS precipitation + FLDAS soil moisture; (c) CRU precipitation + GLDAS soil moisture; (d) GPCC precipitation + FLDAS soil moisture.
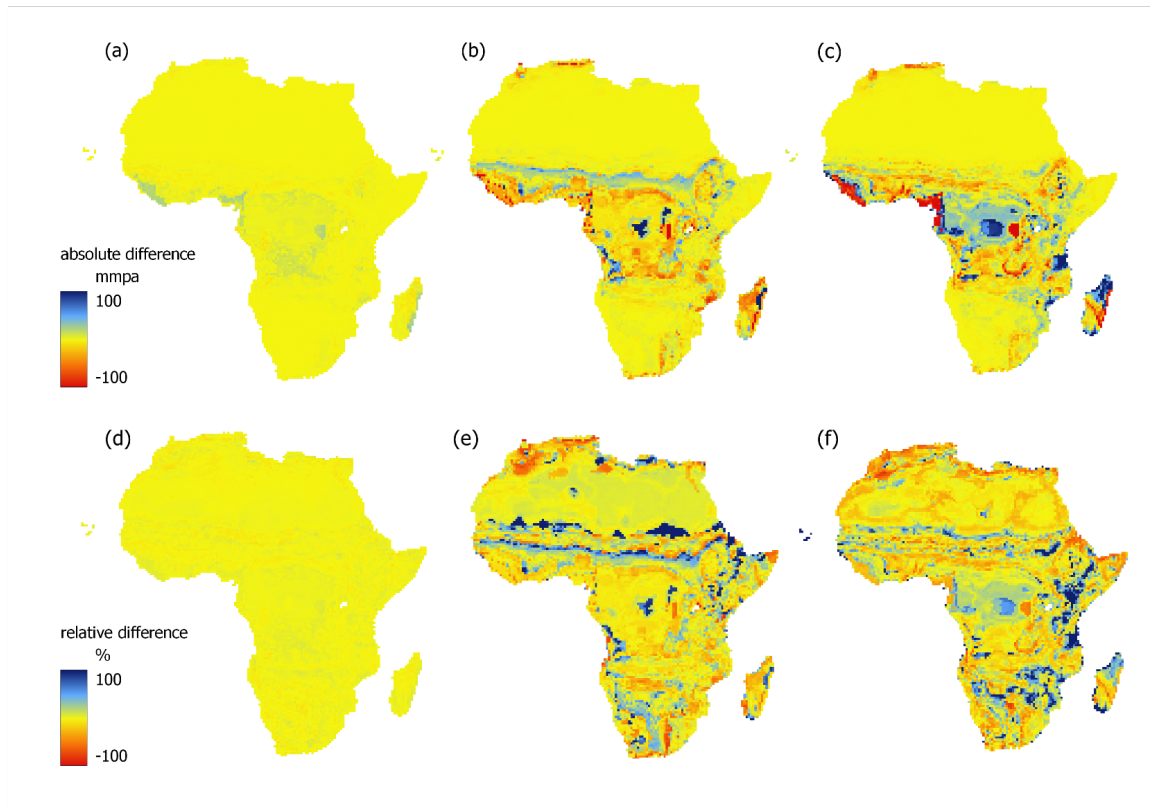
Figure S9. Absolute (top row) and relative (bottom row) spatial differences in modelled groundwater recharge using different precipitation and soil moisture datasets at 0.5° spatial resolution in relation to the base CRU/FLDAS model: CHIRPS precipitation + FLDAS soil moisture (a)/(d), CRU precipitation + GLDAS soil moisture (b)/(e), GPCC precipitation + FLDAS soil moisture (c)/(f).
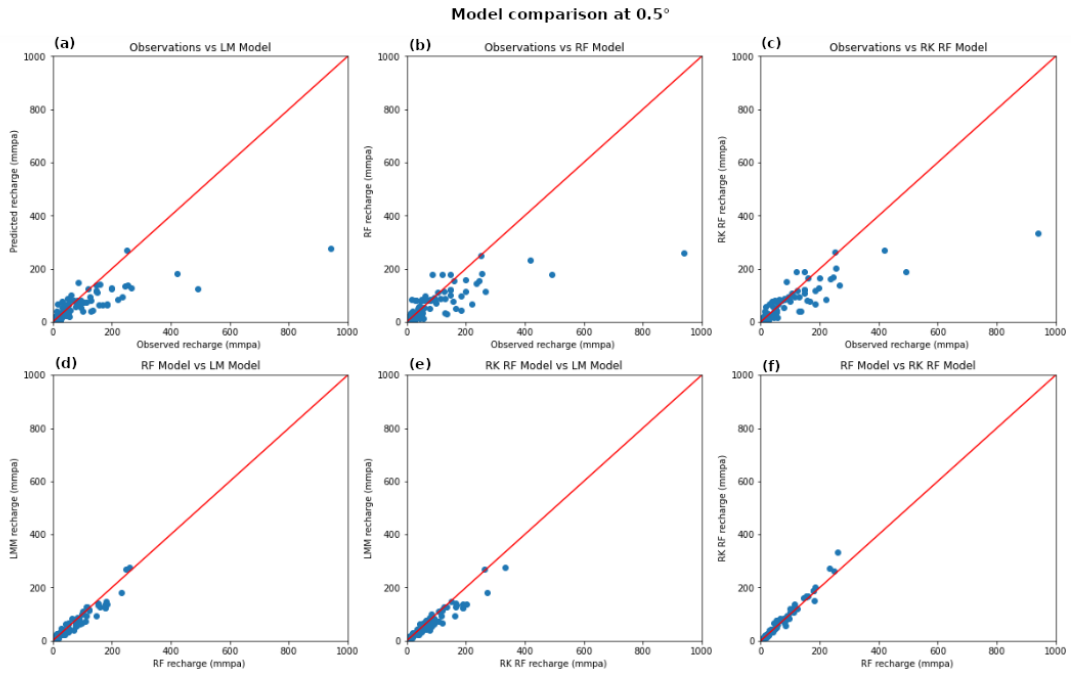
5.3. Fit of the RF models

Figure S10. Plots relating the observed groundwater recharge to the predicted values at 0.5° obtained using the linear mixed model by MacDonald et al. (2021) (a), random forest model (b) and random forest model with residual kriging (c). Their results are compared in (d)-(f).
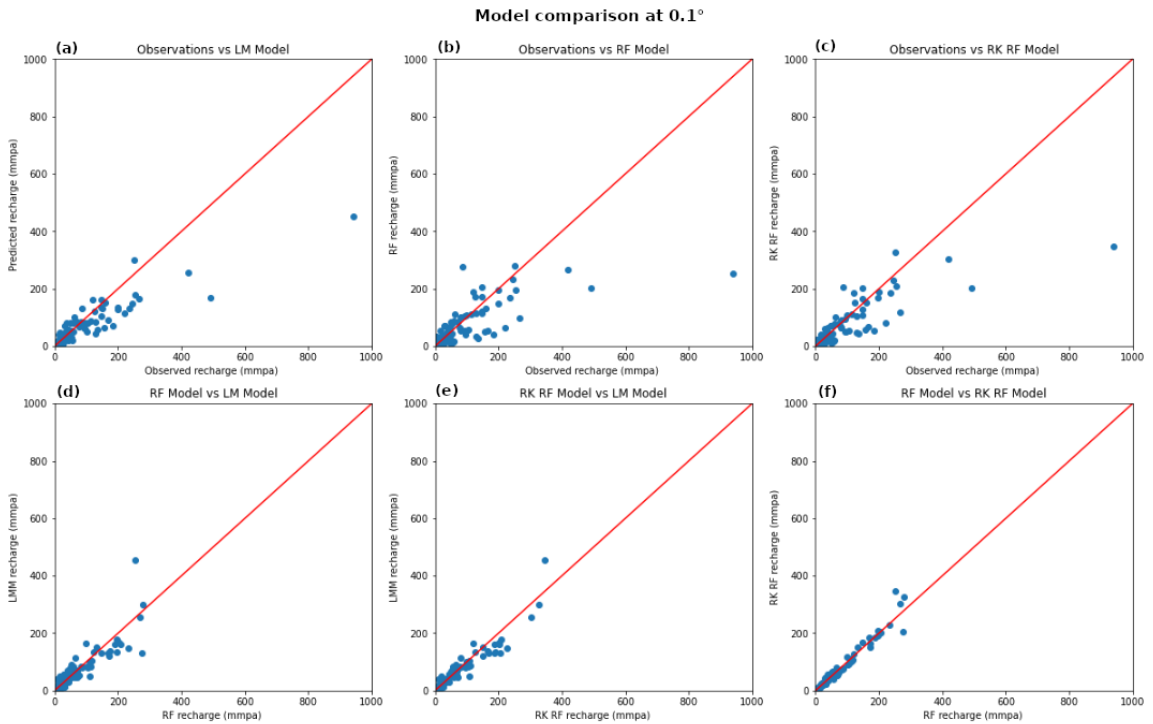

Figure S11. Plots relating the observed groundwater recharge to the predicted values at 0.1° spatial resolution obtained using the linear mixed model developed in this study (a), random forest model (b) and random forest model with residual kriging (c). Their results are compared in (d)-(f).
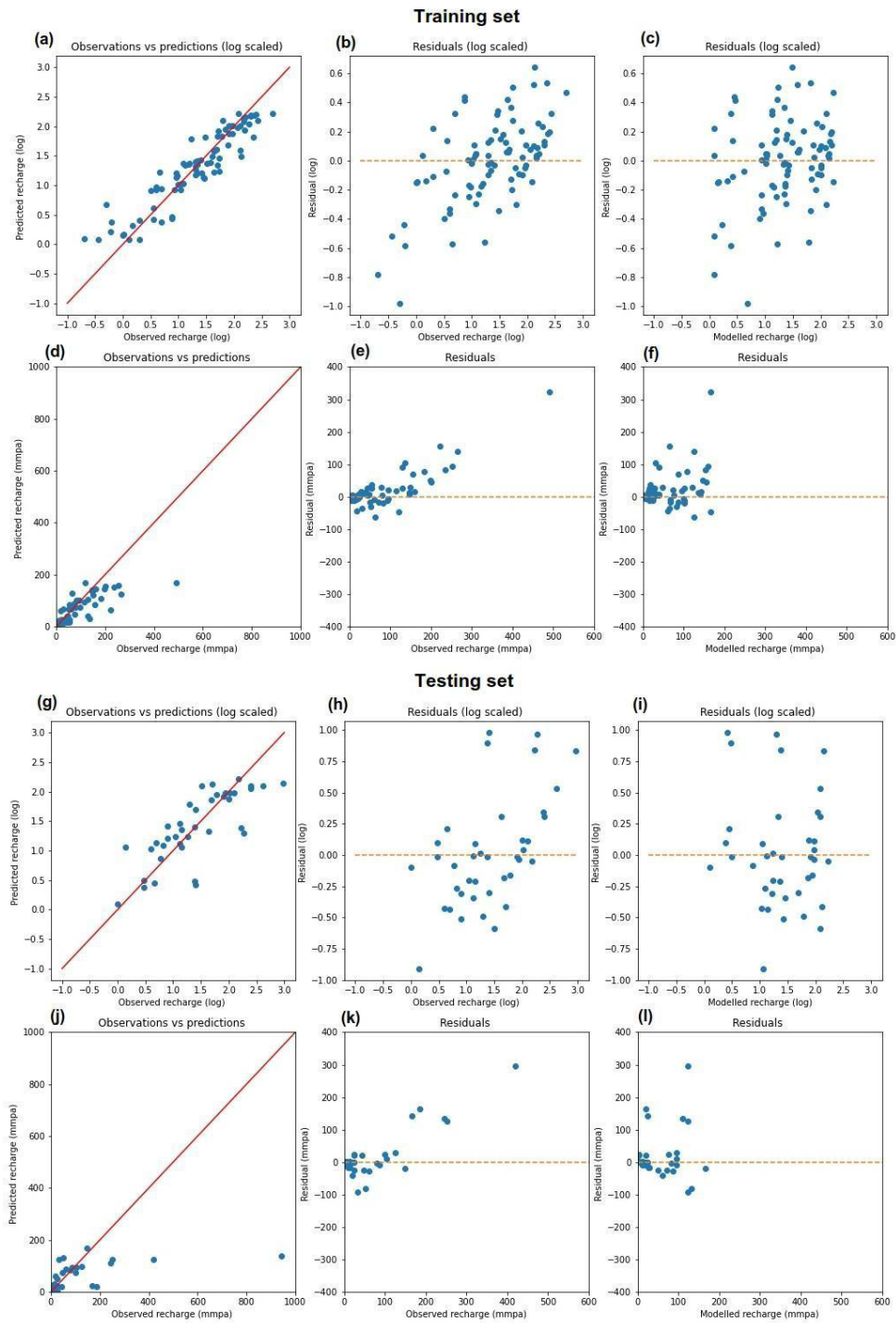
Figure S12. Plots relating the observed and modelled values to model residuals for the training and testing dataset of a <u>randomly selected model</u> in the model series after hyperparameter tuning, at 0.5° spatial resolution. Column 1 presents the observed and modelled recharge values in the log scale (a,g) and in the original scale (d,j). The model residuals are shown in relation to the observed recharge (column 2) and the modelled recharge (column 3) in the log scale (row 2) and in the original scale (row 4). Residual plots leave out high recharge values for better readability. High recharge values are mostly underestimated in both sets, as there are only a few measurements in the areas of high precipitation and high recharge. Thus, the residuals increase with increasing recharge as evident in the segments (f) and (l) illustrating the predicted recharge and the corresponding residuals in the training and testing set respectively. Also, some low recharge values are overestimated on a relative scale.

6.   References

Arino O, Gross D, Ranera F, Bourg L, Leroy M, Bicheron P, Latham J, Di Gregorio A, Brockmann C, Witt R, Defourny P, Vancutsem C, Herold M, Sambale J, Achard F, Durieux L, Plummer S, Weber J. GlobCover: ESA Service for Global Land Cover from MERIS. In Conference Proceedings: Proceedings of the IEEE International Geoscience and Remote Sensing Symposium. Piscataway (United States of America): IEEE-Inst Electrical Electronics Engineers Inc.; 2007. p. 2412-2415. JRC49403

Beaudoing, H., & Rodell, M.:. GLDAS Noah Land Surface Model L4 monthly 0.25 x 0.25 degree V2.0. https://doi.org/10.5067/9SQ1B3ZXP2C5, 2019.

De Vries, J. J., & Simmers, I. : Groundwater recharge: An overview of processes and challenges. Hydrogeology Journal, 10 (1), 5-17, 2002.

Didan, K., Munoz, A. B., Solano, R., & Huete, A.: MODIS vegetation index user's guide (MOD13 series). University of Arizona: Vegetation Index and Phenology Lab, 2015.

Funk, C., Shukla, S., Hoell, A., and Livneh, B.: Assessing the Contributions of East African and West Pacific Warming to the 2014 Boreal Spring East African Drought, Bulletin of the American Meteorological Society, 96, S77–82, https://doi.org/10.1175/BAMSEEE_2014_ch16.1, 2015.

Hartmann, A., Gleeson, T., Wada, Y., & Wagener, T.: Enhanced groundwater recharge rates and altered recharge sensitivity to climate variability through subsurface heterogeneity. Proceedings of the National Academy of Sciences, 114 (11), 2842-2847, https://doi.org/10.1073/pnas.1614941114, 2017

Harris, I., Osborn, T. J., Jones, P., and Lister, D.: Version 4 of the CRU TS monthly high-resolution gridded multivariate climate dataset, Scientific Data, 7, 109, https://doi.org/10.1038/s41597-020-0453-3, 2020.

Jarvis, A., Reuter, H., Nelson, A., & Guevara, E.: Hole-lled SRTM for the globe Version 4, 2008.

Jones A. et al., Soil atlas of Africa. Luxembourg, GD Luxembourg: Publications Office of the European Union, 2013.

Lark, R., Cullis, B., and Welham, S.: On spatial prediction of soil properties in the presence of a spatial trend: the empirical best linear unbiased predictor (E-BLUP) with REML, European Journal of Soil Science, 57, 787–799, 2006.

MacDonald, A. M., Bonsor, H. C., Dochartaigh, B. E. O., & Taylor, R. G.: Quantitative maps of groundwater resources in Africa. Environmental Research Letters, 7 (2), 024009, 2012.

MacDonald, A. M., Lark, R., Taylor, R., Abiye, T., Fallas, H., Favreau, G., Goni, I., Kebede, S., Scanlon, B., Sorenson, J., Tijani, M., Upton, K., & West, C.: Groundwater recharge in Africa from ground-based measurements [British Geological Survey. (Dataset), https://doi.org/10.5285/45d2b71c-d413-44d4-8b4b-6190527912], 2020.

MacDonald, A. M., Lark, R., Taylor, R., Abiye, T., Fallas, H., Favreau, G., Goni, I., Kebede, S., Scanlon, B., Sorensen, J., Tijani, M., Upton, K., & West, C.: Mapping groundwater recharge in Africa from ground observations and implications for water security. Environmental Research Letters, 16, 034012. https://doi.org/10.1088/1748-9326/abd661, 2021.

McNally, A.: FLDAS Noah Land Surface Model L4 Global Monthly 0.1 x 0.1 degree (MERRA-2 and CHIRPS). https://doi.org/10.5067/5NHC22T9375G, 2018.

Mohan, C., Western, A. W., Wei, Y., & Saft, M.: Predicting groundwater recharge for varying land cover and climate conditions - a global meta-study. Hydrology and Earth System Sciences, 22 (5), 2689-2703. https://doi.org/10.5194/hess-22-2689-2018, 2018.

Parr, T., Turgutlu, K., Csiszar, C., & Howard, J. (2018). Beware default random forest importances [Accessed on 28.07.2021]. https://explained.ai/rf-importance/

Schneider, U., Becker, A., Finger, P., Meyer-Christoer, A., Rudolf, B., & Ziese, M.: GPCC Full Data Reanalysis Version 6.0 at 0.5°: Monthly Land-Surface Precipitation from Rain-Gauges built on GTS-based and Historic Data. https://doi.org/10.5676/DWD GPCC/FD M V6 050, 2011.

Trabucco, A., & Zomer, R.: Global Aridity Index and Potential Evapotranspiration (ET0) Climate Database v2. gshare. Fileset. https://doi.org/10.6084/m9.figshare.7504448.v3, 2019.